FACTA UNIVERSITATIS
Series: **Electronics and Energetics** Vol. 38, Nº 3, September 2025, pp. 513 - 531
https://doi.org/10.2298/FUEE2503513A

Original scientific paper

DESGIN DEVELOPMENT AND SIGNAL PROCESSING OF 5G MIMO ANTENNA ON TWO DISTINCT SUBSTRATES

Neetu Agrawal[1], Sanjay Chouhan[2]

[1]Department of Electronics and Communication Engineering, GLA University, Mathura, U.P., India

[2]Department of Electronics and Communication Engineering, Jawaharlal Institute of Technology (JIT) Borawan, M.P., India

ORCID iDs:	Neetu Agrawal	https://orcid.org/0000-0002-0448-9507
	Sanjay Chouhan	https://orcid.org/0000-0003-2654-3567

Abstract. *This article covers the design, development, and signal processing of a 5G mm-wave MIMO antenna. The antenna design is first simulated using CST 18 software and optimized iteratively to meet the requirements. After finalizing the design, a prototype is fabricated and tested in an Anechoic Chamber to measure radiation patterns and gain in a controlled environment. The antenna uses two substrate materials: Rogers RT/Duroid and FR4. Rogers RT/Duroid offers higher efficiency, gain, and lower loss at high frequencies compared to FR4. The design features a partial ground plane and orthogonal positioning of radiating components to enhance isolation. The antenna is designed to be compact and provide high bandwidth, making it ideal for 5G applications. The isolation between ports is greater than 13 dB for the Rogers RT/Duroid substrates and greater than 16 dB for the FR4 substrates. The antenna design using Rogers RT/Duroid resonates at 20 GHz, while the one using FR4 substrates resonates at 28 GHz. Key performance parameters for both substrates, such as ECC (Envelope Correlation Coefficient), MEG (Mean Effective Gain), DG (Diversity Gain), CCL (Channel Capacity Loss), gain, radiation pattern, total and radiation efficiencies, are compared. For the RT/Duroid design, the ECC is less than 0.007, DG is greater than 9.97, CCL is less than 0.4 bps/Hz, peak gain is 7.5 dB, radiation efficiency ranges from 82% to 88%, and total efficiency ranges from 62% to 82% within the desired frequency band (15–35 GHz). In contrast, the FR4 design shows an ECC of less than 0.006, DG greater than 9.95, CCL less than 0.4 bps/Hz, peak gain of 5.6 dB, radiation efficiency between 40% and 52%, and total efficiency between 35% and 50%. RT/Duroid has a relative permittivity (εr) of 2.2, loss tangent (tanδ) of 0.0009, and a thickness (t) of 0.8 mm, while FR4 has an εr of 4.3, tanδ of 0.025, and thickness of 1.6 mm. The efficiency, gain, and return loss limitations can be mitigated by carefully selecting the dielectric material.*

Key words: *MIMO antenna, 5G, ECC, MEG, CCL*

Received December 12, 2024; revised March 16, 2025 and April 01, 2025; accepted April 15, 2025
Corresponding author: Neetu Agrawal
GLA University, Mathura, U.P., India
E-mail: neetuagrawal.ec@gla.ac.in

1. INTRODUCTION

The rapid increase in the use of smartphones, tablets, and Wi-Fi hotspots, coupled with the growing demand for mobile data, has posed significant challenges for wireless service providers in managing the global bandwidth shortage. Providers are striving to deliver high quality, low-latency, and high-resolution data services to mobile devices. Meanwhile, the need for smaller and more portable devices has added complexity to current wireless communication systems. The existing frequency spectrum is also becoming overcrowded due to overlapping technologies, which further complicates the situation. As a result, researchers are exploring new solutions, such as 5G technology and the mm-wave frequency spectrum (30-300 GHz), to tackle these emerging issues. [1]. This paper explores various MIMO antenna designs for 5G communication, including a dual-band antenna for 28/38 GHz mm-wave systems using high isolation metamaterials, as well as a pentagon-shaped antenna that offers wide dual-band performance. [2]. This paper discusses a MIMO antenna designed for 5G mm-wave applications at 28/38 GHz, featuring a compact size, high gain, and wide bandwidth. To reduce mutual coupling between the radiating elements, a parasitic element with a simple geometry is positioned between the MIMO elements. The presence of the parasitic element improves the antenna's isolation, achieving a 25 dB enhancement in isolation [3]. A simulation of several antenna designs over the operating band 10–15 GHz has been carried out. For a variety of substrate materials, return losses, VSWR, and gain was investigated, and their effects were examined [4]. A micro-strip patch antenna with a reverse U-shaped slot operates in two bands at mm-wave frequencies (28 and 38 GHz) [5]. A small MIMO antenna design and characterization for potential 5G applications is presented. The proposed work's unit element is modeled after a typical circular patch antenna, but it has two rectangular slots added to it to provide broad bandwidth and operates a 5G mm band. A defective ground structure is made to improve the antenna's radiating properties and the arrays are rectangular slotted patch antennas [6-7]. A ꝏ-shaped MIMO antenna is introduced for future 5G mm wave communication, resonating at 28 GHz. The proposed MIMO antenna consists of four antenna elements, each spaced 90 degrees apart. Each antenna element's radiating component is made up of four circular ring patches, which play a key role in achieving the desired frequency band operation [8-9]. The bandwidth enhancement of an antenna can be achieved through the frequency-dependent properties of polymer composite dielectric materials [10]. This research demonstrates a combined four-element 5G/4G MIMO antenna system. It operates in the tri-bands of 28/37/39 GHz for 5G and in the 1.8-2.6 GHz band for 4G [11]. This article introduces a multiband MIMO antenna for a 5G system. The proposed antenna is designed using characteristic mode analysis. The planar Inverted-F antenna (PIFA) structure covers the 3.5, 4.3, 28, and 35 GHz bands. [12]. The article has a detailed discussion of design approaches, performance parameter-based optimization, construction, and diversity analysis of the suggested 5G MIMO antenna. The elliptical slot is crucial to the design to attain high bandwidth [13]. The purpose of this research was to create a compact MIMO antenna that has a large coverage area, and provides strong isolation properties over the necessary resonance bandwidth. The presented antenna has a straightforward design, has a wideband performance of nearly 15 GHz, and has superior isolation of 26 dB. The addition of a line resonator has increased the isolation level [14]. This paper presents a compact four-port MIMO antenna designed for 5G applications. The antenna has a size of 11.3 mm *31 mm, excluding the feed lines [15]. A single-element array with a 2:1 Voltage Standing Wave Ratio (VSWR) is designed on a Rogers RT Duroid 5880 substrate, targeting the 27.06–28.35 GHz frequency range for 5G applications [16]. This paper presents the design and implementation of a compact MIMO antenna system, featuring Coplanar Waveguide (CPW) feeding and a connected ground structure [17].

This paper introduces an S-shaped, four-port Multiple Input Multiple Output (MIMO) wideband mmWave antenna, operating within the 25 GHz to 39 GHz frequency range [18]. A wideband antenna incorporating double negative (DNG) metamaterial has been designed and analyzed for use in both 4G and 5G applications [19]. This paper introduces a compact multi-slotted patch antenna designed for Long-Term Evolution (LTE) and 5G communication applications. The proposed antenna features a stepped patch along with a ground plane. [20]. A planar rectangular slot antenna with dual-band functionality and enhanced peak gain has been proposed, designed, and manufactured for sub-6 GHz 5G applications [21]. On FR4 substrates, a dual-element octagon antenna with a slot is created that operates between 3.1-4.5 GHz in the 5G sub-6 GHz spectrum. To minimize mutual coupling between MIMO antennas, an isolation element of T shape is positioned at the ground plane. The physical dimensions of the MIMO antenna are 55*38 mm2, and its ECC (or correlation) value across the completely operational spectrum is 0.0004 [22]. To improve isolation and better match impedance, a modified T-shape stub was kept between radiators and used modify tapered feedline with a defective ground structure in a 20*35 mm2 MIMO antenna array for n78/ 3.3-3.8 GHz, 5G band. In the operating band, the antenna produced a gain of 2.34 dBi and a radiation efficiency of 93% [23]. Compact MIMO antennas of different shapes are designed on FR4 substrate in a low operational frequency band using improved isolation techniques [24-27]. There are numerous antennas and antenna arrays designs with different isolation techniques were studied [28-29]. This paper presents a broadband antenna array designed for 28 GHz 5G communication. The array measures 45 * 20 mm² and operates within the frequency range of 25.052–34.923 GHz, as confirmed by measurements [30]. Most of the researcher has designed MIMO antenna on FR4 substrate for low band (<6 GHz) and on RT/Duroid for mm-wave band (>6GHz) 5G application.

The proposed dual band MIMO antenna consists of a rectangular ground plane on one side of the substrate and an F-shaped radiator with a circular slot in the middle [31, 34]. A novel low power beamforming method for Massive MIMO systems is presented in this research. [32]. A MIMO wideband 3D antenna system with 8 ports in an octagon form is proposed in this article for terahertz (THz) applications. The proposed MIMO antenna systems are suitable for sixth-generation wireless communication networks [33]. At the mm-wave band, FR4 is not ideal due to its low gain and efficiency, although it is more affordable than RT/Duroid. This paper presents the design of a MIMO antenna on both FR4 and RT/Duroid substrates and compares their performance. FR4 provides better return loss and good isolation, while RT/Duroid offers higher gain, greater efficiency, improved ECC and DG, and a better radiation pattern in the mm wave 5G band. Therefore, RT/Duroid is a superior substrate for the mm-frequency band.

2. MIMO Antenna Design

The proposed MIMO antenna is fabricated using two dielectric materials: FR4 and Rogers RT/Duroid 5880. The permittivity (εr), tangent loss ($\tan\delta$), and thickness (t) for the FR4 substrate are 4.3, 0.025, and 1.6 mm, respectively, while for the RT/Duroid substrate, they are 2.2, 0.0009, and 0.8 mm. While Rogers RT/Duroid is a less lossy substrate compared to FR4, it is more expensive. The schematic Top view and back view structure of the proposed MIMO antenna with optimized dimensions is shown in Figure 1(a) and design steps of single antenna,

Table 1 Optimize parameters

Antenna Parameters	a=f_l	b	c	d	e	h	i	j	k	l	f_w
Size in millimeter	7.89	5	8	6	2.0	15	15	7.7	30	30	3.8

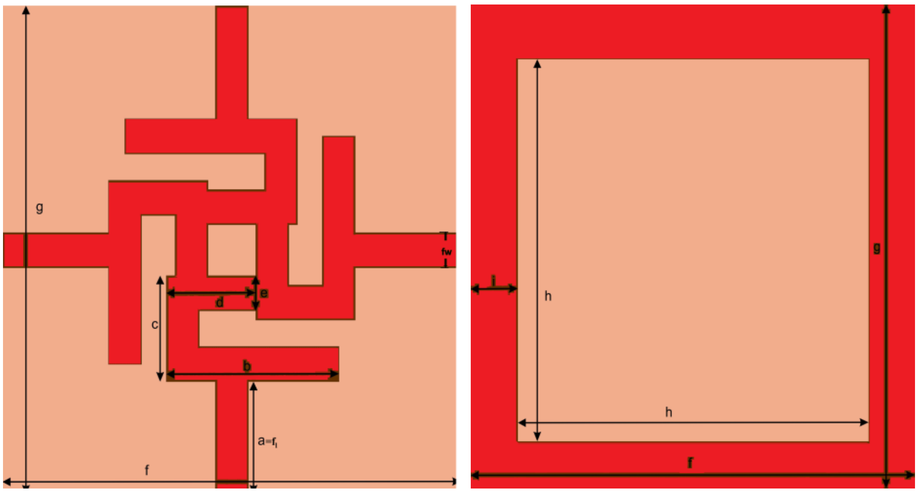

Top View Back View

(a)

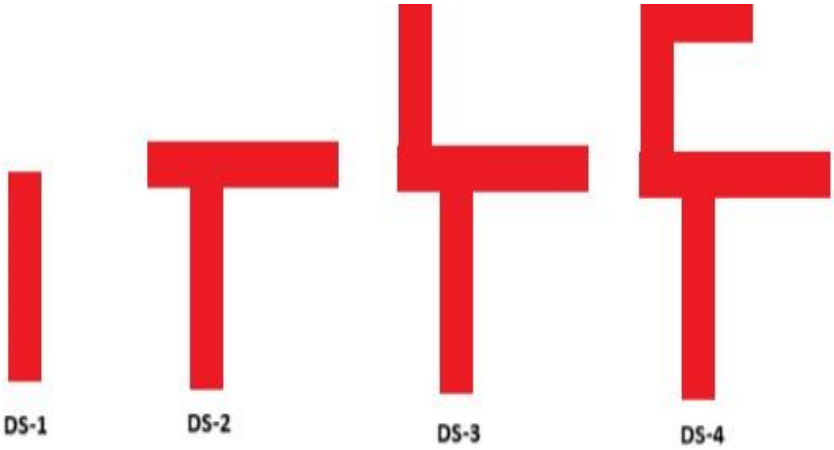

(b)

Fig. 1 Schematic structure of proposed antenna (a) Top View & Back view MIMO (b) Design steps of Single antenna

is shown in Figure 1(b). In Step 1, a 50-ohm meander line is created. Similarly, meander line antennas are developed in steps 2, 3, and 4. Table 1 presents the optimized dimensions of the antenna. The fabrication design of the proposed MIMO antenna for both FR4 and Rogers RT/Duroid 5880 substrates is shown in Figure 2. The substrate size for both antennas is 30 mm * 30 mm, though the thicknesses differ. The front view of the antenna design is identical, with four radiating elements connected to form a common element. In a MIMO system, the antennas are arranged and connected to optimize their S-parameters and resonance frequency. In the bottom view, a ring-shaped ground plane is used to reduce size and enhance isolation. The ring-shaped ground plane is created by a square cut of 22 mm * 22 mm for the FR4 design and 15 mm *15 mm for the Rogers RT/Duroid 5880 design within the full ground plane. The substrate material is placed between the radiating elements and the ground plane in the patch antenna. Both the radiating elements and ground plane are made of perfect electrical conductor (PEC) material. A meandered line structure is employed to compact the antenna, and the shared geometry provides a wide bandwidth and improves gain. The proposed shared meandered MIMO antenna is more compact and delivers improved performance. A 50 Ω SMA connector was used at the input port to feed the radiator. The specifications of the substrates for the FR4 and Rogers RT/Duroid designs are provided in Table 2.

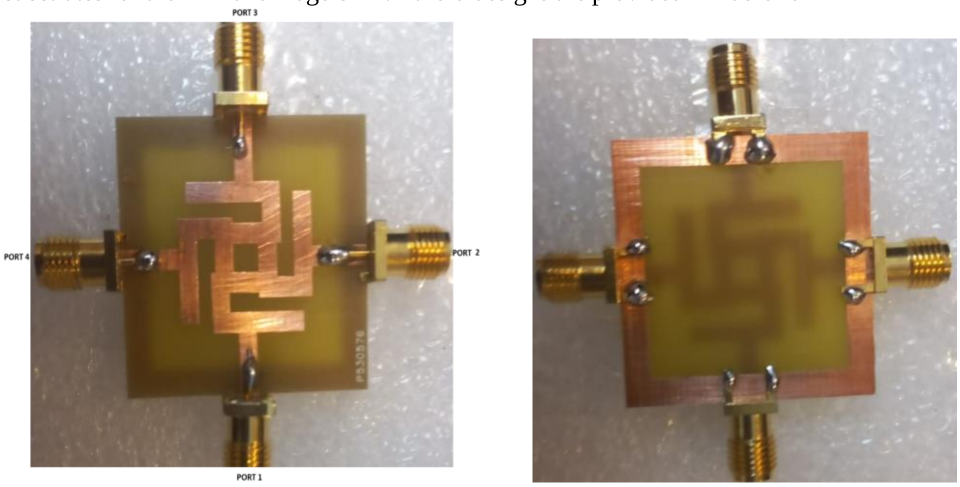

Top View Back View

(a)

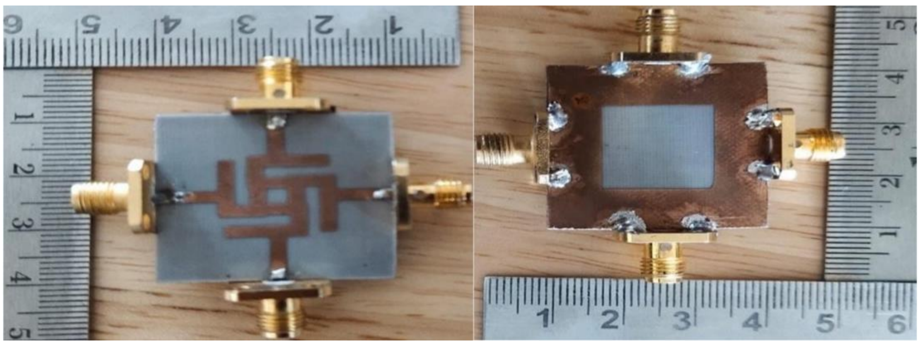

Top View Back View

(b)

Fig. 2 Fabrication design of MIMO antenna for (a) FR4 (b) Rogers RT/Duroid

Table 2 Substrates specification of design MIMO antenna

Parameter	FR4	RT/duroid 5880
Substrate thickness	1.6 mm	0.8mm
Permittivity and tangent loss	$\varepsilon_r = 4.3$, $\tan\delta = 0.025$	$\varepsilon_r = 2.2$, $\tan\delta = 0.0009$
Ground cut (mm^2)	22*22	15*15
Overall size (mm^2)	30*30	30*30

3. Result and Discussion

The CST-18 version Studio Suite software was used for simulation and a ZNB20 vector network analyzer (VNA) was used to measure the S-parameters of the proposed MIMO antenna for both substrates (FR4 and Rogers RT/Duroid). The reflection and isolation coefficients were analyzed using the S-parameters. The reflection coefficient is represented by S11, while the isolation coefficients are represented by S21, S31, and S41. Figure 3 shows the measured and simulated reflection coefficient (S11) for both FR4 material and Rogers RT/Duroid polymer.

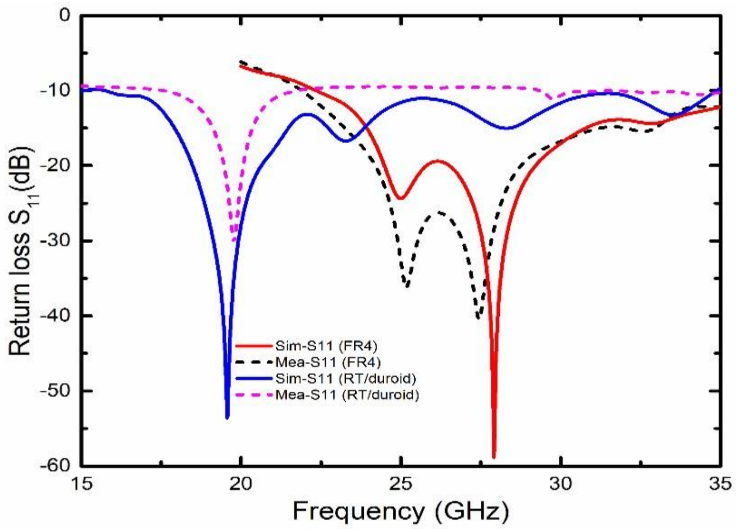

Fig. 3 Return loss S_{11} results for FR4 and Rogers RT/Duroid

The measured frequency range of the proposed MIMO antenna for Rogers RT/Duroid is 17.56-21.76 GHz, while the simulated frequency range is 15.74-34.88 GHz. The simulated return loss at the 19.7 GHz resonance frequency is 55 dB, and the observed return loss at the 20 GHz resonance is 30 dB. Similarly, the measured frequency range of the proposed MIMO antenna for FR4 is 22.3-35 GHz, while the simulated frequency range is 22-35 GHz. The simulated return loss at the 27.4 GHz resonance frequency is 59 dB, and the observed return loss at the 27.9 GHz resonance is 42 dB. Slight variations between the measured and simulated results are attributed to manufacturing errors. Measured and simulated isolation coefficients (S21, S31, S41) for FR4 and Rogers

RT/Duroid are shown in Figure 4 (a) and 4(b) respectively. The simulated and measured isolation is below -13 dB in the operating band of 15-35 GHz for Rogers RT/Duroid, while for the FR4 design, the isolation is below -16 dB. Table 3 presents the result comparisons for both substrate designs (FR4 and RT/Duroid) within the operating band of 15-35 GHz.

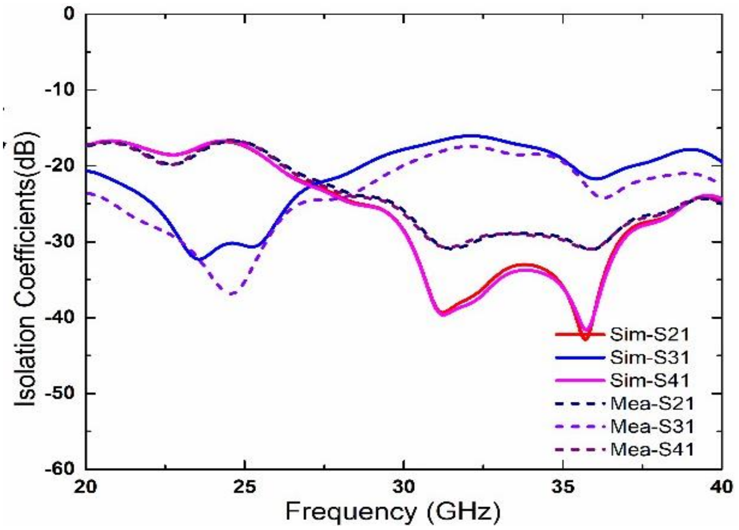

(a)

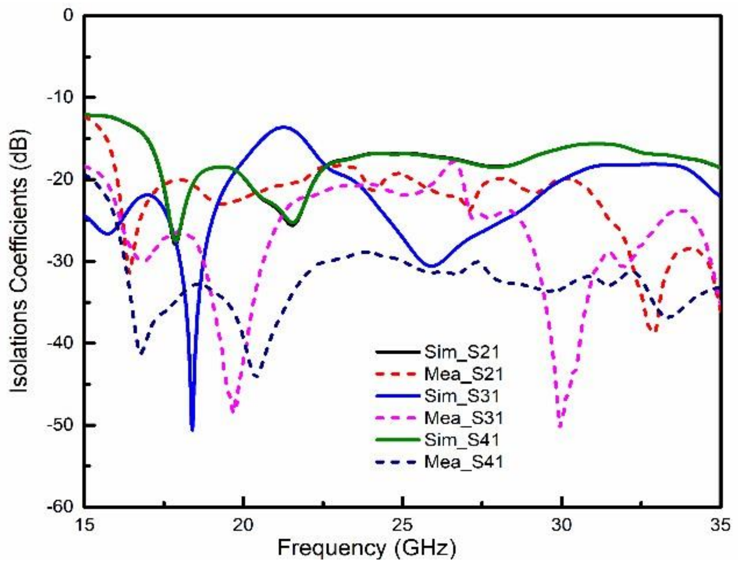

(b)

Fig. 4 Isolation results for (a) FR4 (b) Rogers RT/Duroid

Table 3 Result comparisons for FR-4 and RT/Duroid

Parameters result	FR4 Design	Rogers RT /Duroid
Return loss	59 dB	55dB
Resonance frequency	28 GHz	20 GHz
Isolation	<-16 dB	<-13 dB
Peak gain	5.6 dBi	7.5 dBi
ECC	0.0012	0.007
DG	>9.94 dB	>9.97 dB
Radiation efficiency	>36%	>82%
Total efficiency	>32%	>62%
MEG	<-3dB	<-2.8dB
SCD	78.1Amp/m	281 Amp/m

The surface current distribution (SCD) of the proposed antenna for both FR4 and Rogers RT/Duroid is shown in Figure 5. For the surface current analysis, port 1 is excited, while the other ports are terminated with matching impedance. The analysis shows a reduced current coupling with antenna elements 2, 3, and 4. At different ports, the surface current ranges from 0 to 78.1 A/m for FR4, and from 0 to 281 A/m for Rogers RT/Duroid. The effects of coupled return loss and isolation factors are analyzed using the Envelope Correlation Coefficient (ECC).

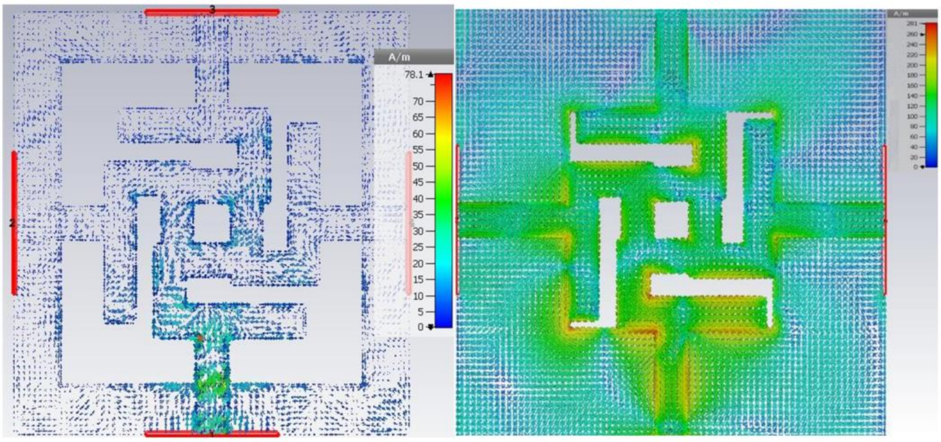

(a) (b)

Fig. 5 Surface current distribution results for (a) FR4 (b) Rogers RT/Duroid

Figure 6 shows the measured and simulated ECC results for the FR4 and Rogers RT/Duroid systems. The simulation and measurement results indicate that the ECC is less than 0.0012 for the FR4 design, and less than 0.007 for the Rogers RT/Duroid design across the entire simulated frequency range, demonstrating the effectiveness of the MIMO antenna's diversity performance. The ECC values suggest minimal correlation between the antenna elements. S-parameters can be used to determine the ECC, which represents the relationship between antenna elements. ECC is particularly important in this context, as individual isolation measurements cannot fully capture the diversity response.

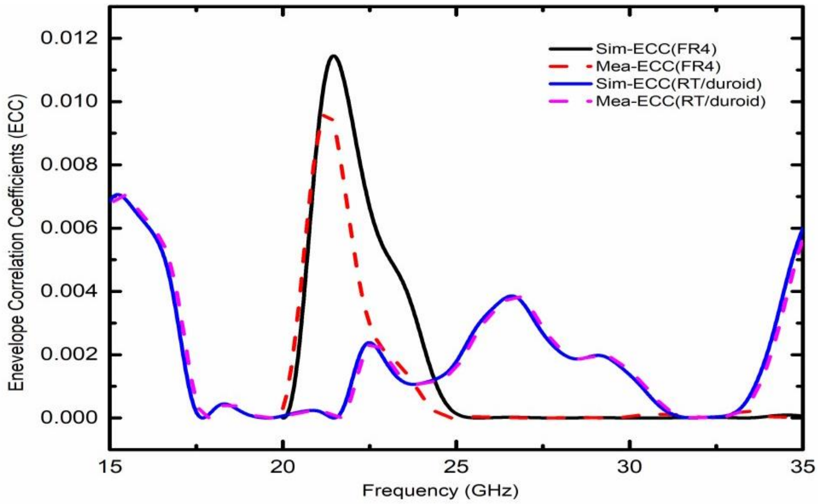

Fig. 6 ECC results for FR4 and Rogers RT/Duroid

The diversity gain (DG) of the proposed MIMO antenna for FR4 and Rogers RT/Duroid is shown in Figure 7. For the FR4 design, the DG exceeds 9.95 dB across the entire frequency range, while for the Rogers RT/Duroid design, the DG exceeds 9.97 dB. The ideal DG value is 10 dB. As the DG increases, the correlation value decreases Rogers RT/Duroid.

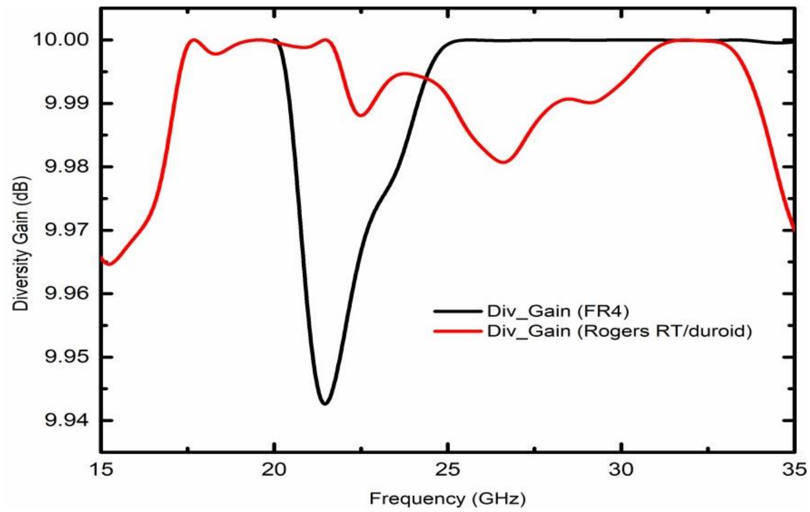

Fig. 7 Diversity gain result for FR4 and Rogers RT/Duroid

The MEG (Maximum Efficiency Gain) can be used to highlight the diverse aspects of MIMO antennas. To evaluate the MEG's diversity performance for different cross-polarization ratios (XPR), it is analyzed for two mediums: isotropic and Gaussian. The MEG values for both isotropic and Gaussian mediums are shown in Figure 8. A comparison of the various MEG values at the resonance frequency is presented in Table 4

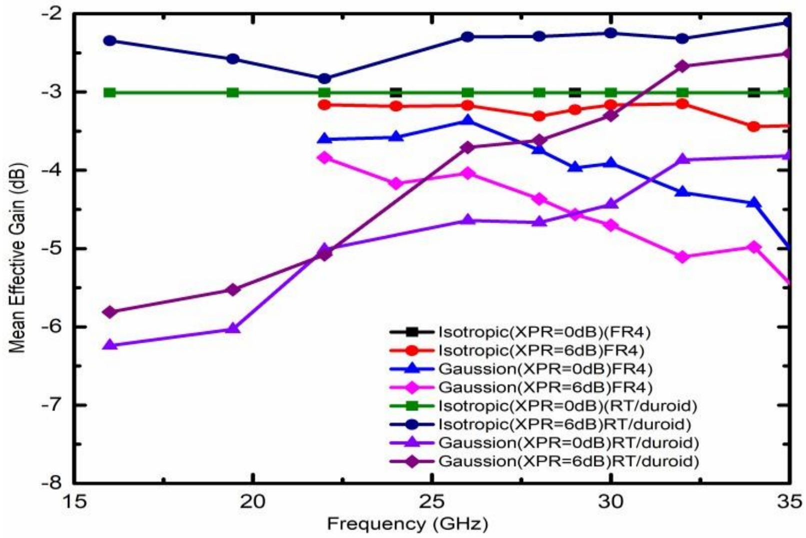

Fig. 8 Mean effective gain result for FR4 and Rogers RT/Duroid at isotropic and Gaussian medium

Table 4 MEG result at a resonance frequency

MEG		Isotropic Medium		Gaussian Medium	
Design	Resonance Frequency (GHz)	XPR=0dB	XPR=6dB	XPR=0dB	XPR=6dB
FR4	28	-3.0	-3.3	-3.8	-4.4
Rogers RT/Duroid	20	-3.3	-2.8	-6.0	-5.5

Figure 9 shows the measured and simulated gain for both the FR4 and Rogers RT/Duroid designs. For the FR4 design, the measured gain ranges from 3.3dB to 4.96 dB, while the simulated gain ranges from 3.4dB to 5.6 dB across the frequency spectrum. The simulated and measured gains at the resonance frequencies are 5.2 dB and 4.96 dB, respectively. For Rogers RT/Duroid, the measured gain ranges from 4.7 to 6.4 dB, while the simulated gain ranges from 3.15 dB to 7.5 dB across the frequency spectrum. At the resonance frequency, the simulated and measured gains are 7.5 dB and 6.2 dB, respectively.

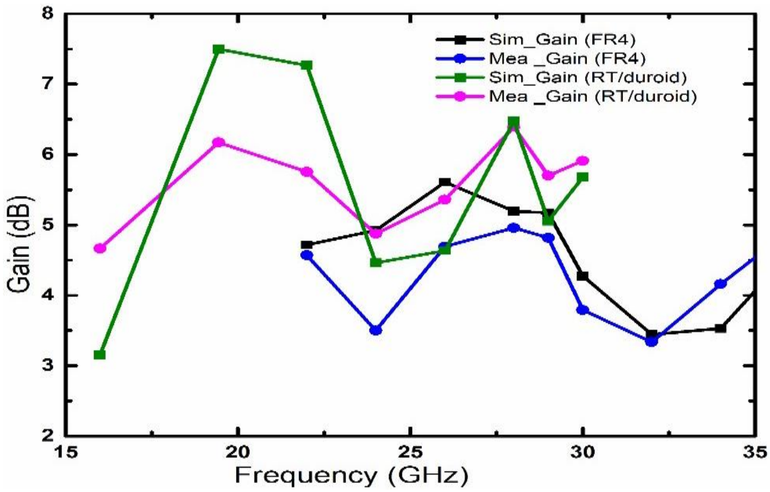

Fig. 9 Gain result for FR4 and Rogers RT/Duroid

Figure 10 shows the measured and simulated efficiency for both Rogers RT/Duroid and FR4. For Rogers RT/Duroid, the radiation efficiency and total efficiency exceed 82% and 62%, respectively. In contrast, for the FR4 design, the radiation efficiency and total efficiency are greater than 38% and 36%, respectively, as shown in Figure 10. CCL (Channel Capacity Loss) was incorporated into the MIMO characteristics to provide insights into the channel capacity losses the system experiences due to correlation. CCL is another important performance metric for MIMO antennas.

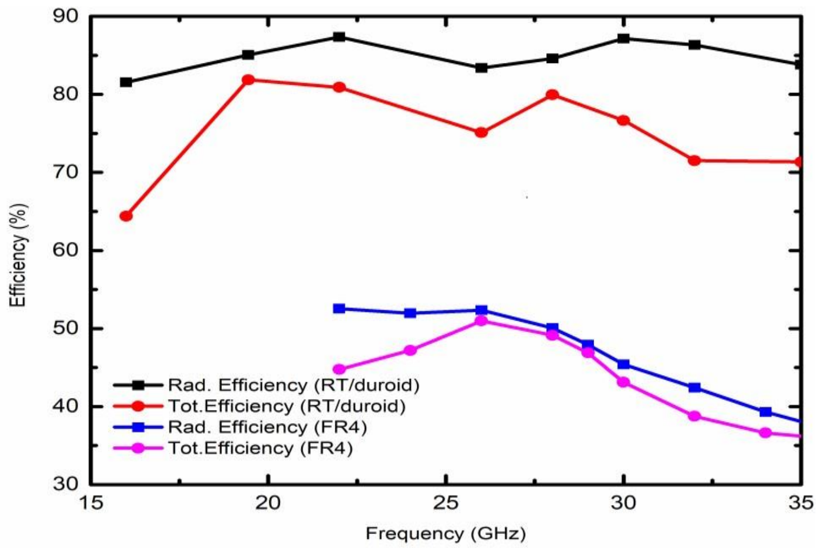

Fig. 10 Efficiency result for FR4 and Rogers RT/Duroid

The CCL results over the frequency spectrum are shown for both FR4 and RT/Duroid in Figure 11. The CCL in the operating bands must be less than 0.4 bps/Hz to meet the specified requirements, as indicated in Figure 11. The radiation patterns for the E-plane and H-plane are shown in Figures 12(a) and 12(b) for FR4, and in Figures 12(c) and 12(d) for RT/Duroid. For FR4, the E-field has a magnitude of 15.2 dBV/m, with the main lobe directed at 335 degrees, while the H-field has a main lobe direction of 135 degrees and a magnitude of 31.9 dBA/m. For RT/Duroid, the E-field has a magnitude of 20.5 dBV/m, with the main lobe directed at 330 degrees, while the H-field has a main lobe direction of 0 degrees and a magnitude of 34.3 dBA/m.

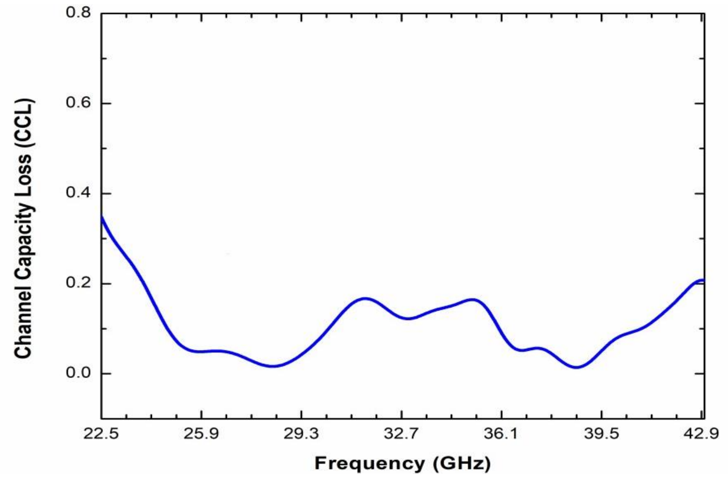

(a)

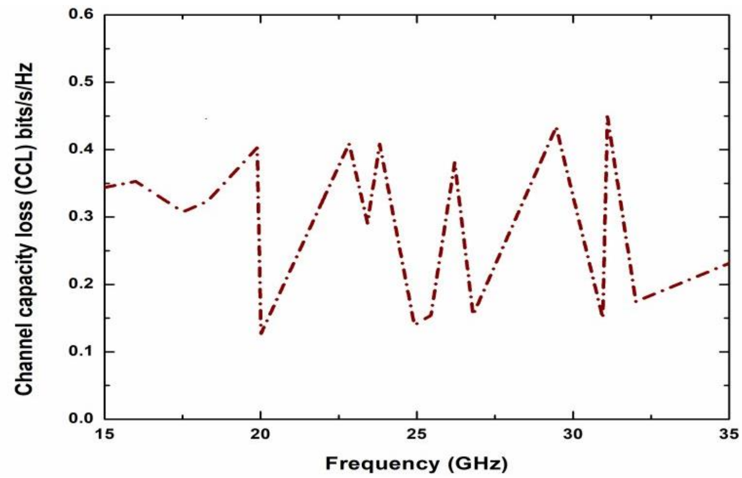

(b)

Fig. 11 CCL result for (a) FR4 (b) RT/Duroid

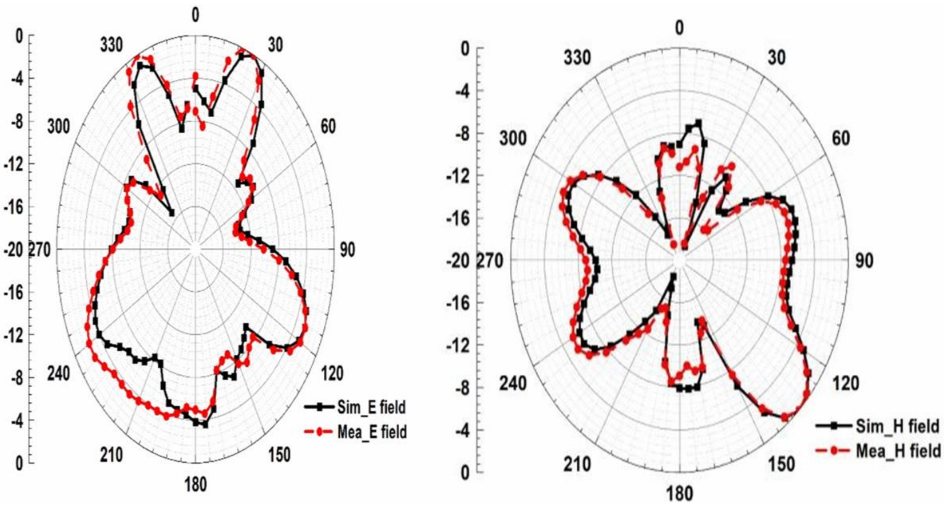

E-plane radiation pattern H-plane radiation pattern

(a)

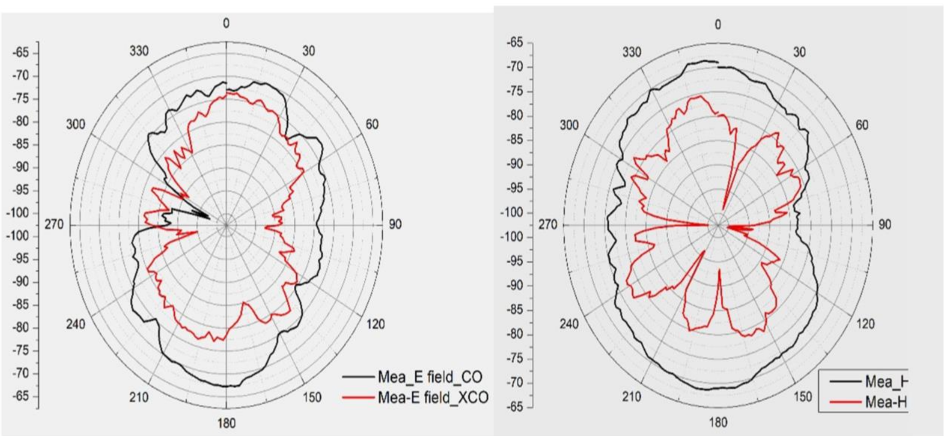

E-plane radiation pattern H-plane radiation pattern

(b)

Fig. 12 Radiation pattern result (a) FR4, (b) RT/Duroid

The parametric analysis is done for varying feed width and feed length of proposed design antenna, are shown in Figures13 (a) and 13(b). The S11 result is observed for feed width 3.6 -4.0 mm and got return loss and sharp resonance at 3.8 mm feed width. Similarly good return loss at 7.89 mm feed length of selected range from 7.69 mm to 8.09 mm.

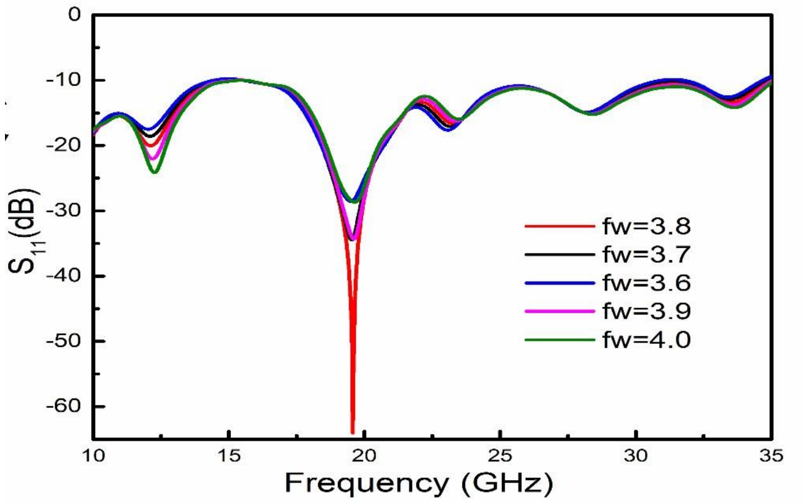

(a)

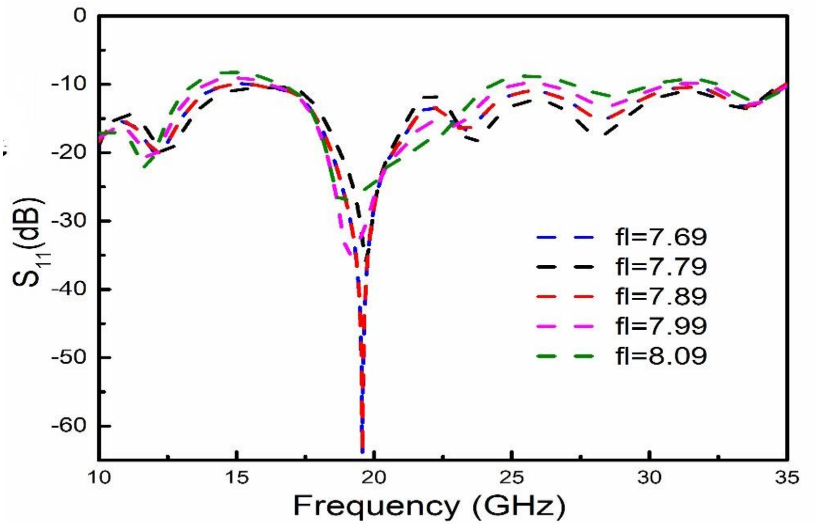

(b)

Fig. 13 Parametric analysis by changing (a) Feed width; (b) Feed length

The effect of full ground plane and partial ground plane on S-parameters are also observed by Figure 14. The partial ground structure antenna is having good result.

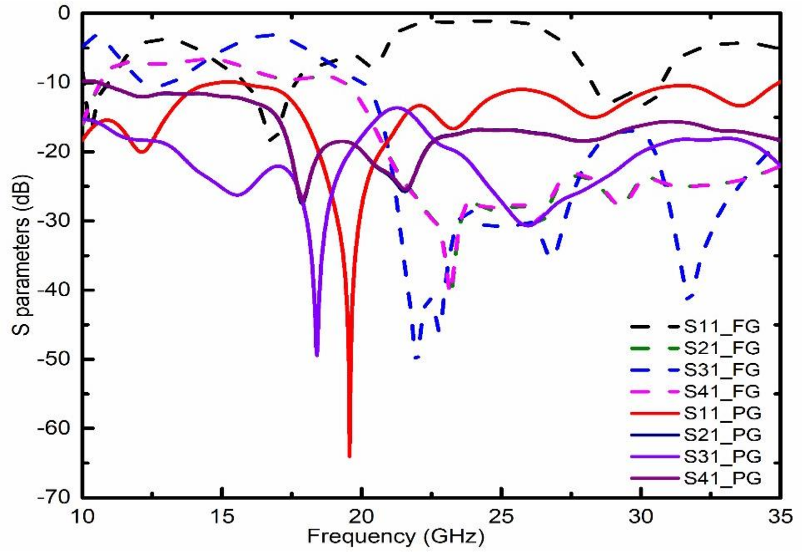

Fig 14 S- parameters result with Full Ground (FG) and Partial Ground (PG) Plane

Table 5 compares the proposed design with various existing 5G antenna designs. The proposed design demonstrates optimum antenna performance characteristics, making it suitable for use in 5G communication. The results from the proposed design and its simulations show that the proposed design includes all these critical metrics.

Table 5 Comparative study with existing state of art literature

Ref	Overall size (mm^2)	Substrates	Resonance freq. (GHz)	Return loss (dB)	Isolation (dB)	Operating band (GHz)
[4]	30*30	Rogers RT5880 ε_r = 2.2, tanδ = 0.0009, t = 1.575mm	27	30	<-29	26.16-29.72
[5]	26*14.5	Rogers RT5880 ε_r = 2.2, tanδ = 0.0009, t = 0.508mm	28 38	22 20	-39 -38	21.4- 29.35, 36.6-40.4
[6]	28*28	Rogers Duroid RT/5870 ε_r = 2.33 tanδ = 0.0012, t = 0.79 mm	28 38	>20	-50	26-31.5, 36.5-41.74
[8]	157.7*70	Rogers RT5880 ε_r = 2.2, tanδ = 0.0009, t = 0.508 mm	28 38	25	>25	27.15-28.77, 37.59-38.49

[10]	30*35	Rogers R04350B, ε_r = 3.66, t = 0.76 mm	28	NG	<-10	25.5-29.6
[15]	48*31	Neltec ε_r = 2.2, tanδ = 0.0009, t = 10 mil	28	>10	>21	26-31
[16]	51.44*18.34	Rogers RT Duroid 5880 ε_r = 2.2, tanδ = 0.0009, t = 0.8 mm	28	>10		27.06-28.35
[17]	24*24	Roger RT/Duroid 5880 ε_r = 2.2, tanδ = 0.0009, t = 0.8 mm	NG	>10	>20	24.8-44.5
[18]	24*24	RO5880 ε_r = 2.3, t = 0.524 mm	29	>10	26	25-39
Proposed work	30*30	FR4 ε_r = 4.3, tanδ = 0.025, t = 1.6 mm	28	58.8	<-16	15-35
		Rogers RT/Duroid ε_r = 2.2, tanδ = 0.0009, t = 0.8 mm	20	53.5	<-13	

Ref	Gain	ECC	Eff. (%)	DG (dB)	CCL (bps/Hz)	MEG	Remark
[4]	7.1	<0.0005	>90	9.999	0.15	<-6	Same size but low gain using same substrate
[5]	5.2 5.5	0.001	92.2 92	9.99	0.05		Placement of metamaterial unit cells is more challenging to design.
[6]	9.5 11.5	0.001	NG	9.99	<0.01		Parasitic element used for reducing mutual coupling. Design and placement of it, is more challenging.
[8]	8.2 8.7	0.001	98 97.6	9.995	NG		By placing the slot, an LPF, the truncated ground, and a meandered line structure is challenging task.

[10]	8.3	<0.01	Nearly 82	>9.96	<0.4	NG	T-junction power combiner/divider feed network is used. It is complicate task.
[15]	10	<15 × 10−4	NG	NG	NG	NG	Trimming the corner of the rectangular high refractive index metamaterial region along with a ground stub between antennas to enhance isolation is tough task.
[16]	16.07	-	>93			<-3	Antenna array is used here. Overall size is more than proposed design.
[17]	8.6	<0.008	>85	>9.5	NG	NG	Coplanar Waveguide (CPW) feeding is used in this paper. Less easy, needs drilling and soldering
[18]	7.1	<0.05	>85	NG	NG	<-3	Decoupling network is used to reduce mutual coupling with compromising ohmic loss.
Proposed work	5.6	0.012	>36 (R.E) >38 (T.E)	>9.94	<0.4	<-3	Defected ground plane and Orthogonal arrangement of antenna element to reduce mutual coupling is more simple technique.
	7.5	0.007	>62 (R.E) >82 (T.E)	>9.97		<-2.8	

Note: *NG (Not given)

4. CONCLUSION

The novelty of this research paper lies in its first-time performance comparison between FR4 and Rogers RT/Duroid antenna designs. Still during the literature survey, no investigation has been carried out regarding the right substrate selection for 5G bands. This was problem that, there was no literature survey on same antenna design with different materials. The key finding of paper provides a detailed analysis and comparison of the two substrates in terms of key performance metrics, such as return loss, gain, efficiency, ECC, MEG, DG, and CCL, highlighting the strengths and limitations of each material in high-frequency applications. By examining these two materials, the study offers new insights into the suitability of FR4 and Rogers RT/Duroid for 5G communication systems, contributing valuable information to the field of antenna design. Substrate FR4 is most suited for Sub-6GHz 5G technology, whereas RT/Duroid is the ideal substrate for offering the greatest performance to build antenna in 5G millimeter wave technology. The FR4 and Rogers RT/Duroid substrates are used to build the suggested antenna, and their comparisons within the operating frequency range of 15–35 GHz are discussed. With same size, proposed antenna, gain is improved by 1.9 dB; radiation efficiency is improved by 26% and total efficiency by 44%, ECC low by 0.005 and more directivity for Rogers's substrate than FR4 substrate.

REFERENCES

[1] S. Jun, Y. Kang, J. Kim and C. Kim, "Ultra-Low-Latency Services in 5G Systems. A Perspective from 3GPP Standards", *ETRI J.*, vol. 42, pp. 721-733, 2020.

[2] T. Nahar and S. Rawat, "Survey of Various Bandwidth Enhancement Techniques Used for 5G Antennas", *Int. J. Microw. Wirel. Technol.*, vol. 14, no. 2, pp. 204-224, 2022.

[3] T. S. Rappaport, S. Sun, R. Mayzus, H. Zhao, Y. Azar, K. Wang, G. N. Wong, J. K. Schulz, M. Samimi and F. Gutierrez, "Millimeter Wave Mobile Communications for 5G Cellular", *IEEE Access*, vol. 1, pp. 335-349, 2013.

[4] M. Hussain, E. M. Ali, S. M. R. Jarchavi, A. Zaidi, A. I. Najam, A. A. Alotaibi, A. Althobaiti and S. S. M. Ghoneim, "Design and Characterization of Compact Broadband Antenna and Its MIMO Configuration for 28 GHz 5G Applications", *Electronics*, vol. 11, no. 4, p. 523, 2022.

[5] B. A. Esmail and S. Koziel, "High Isolation Metamaterial-based Dual-band MIMO Antenna for 5G Millimeter-wave Applications", *AEU-Int. J. Electron. Commun.*, vol. 158, p. 154470. 2023.

[6] M. Hussain, W. A. Awan, E. M. Ali, M. S. Alzaidi, M. Alsharef, D. H. Elkamchouchi, A. Alzahrani, M. F. A. Sree, "Isolation Improvement of Parasitic Element-Loaded Dual-Band MIMO Antenna for Mm-Wave Applications", *Micromachines*, vol 13, no. 11, p. 1918, 2022.

[7] A. Rahim and P. K. Malik, "Analysis and Design of Fractal Antenna for an Efficient Communication Network in the Vehicular Model", *Sustain. Comput.: Inform. Syst.*, vol. 31, p. 100586, 2021.

[8] S. Islam, M. Zada and H. Yoo, "Low-Pass Filter Based Integrated 5G Smartphone Antenna for Sub-6GHz and mm-Wave Bands", *IEEE Trans. Antennas Propag.*, vol. 69, no. 9, pp. 5424-5436, 2021.

[9] M. M. Kamal, S. Yang, X. C. Ren, A. Altaf, S. H. Kiani, M. R. Anjum, A. Iqbal, M. Asif and S. I. Saeed, "Infinity Shell-Shaped MIMO Antenna Array for mm-Wave 5G Applications", *Electronics*, vol. 10, no. 2, p. 165, 2021.

[10] M. Khalid, et al., "4-Port MIMO Antenna with Defected Ground Structure for 5G Millimeter Wave Applications", *Electronics*, vol. 9, no.1, p. 71, 2020.

[11] E. Al-Abbas, M. Ikram, A. T. Mobashsher and A. Abbosh, "MIMO Antenna System for Multi-Band Millimeter-Wave 5G and Wideband 4G Mobile Communications", *IEEE Access*, vol. 7, pp. 181916-181923, 2019.

[12] N. Kumar and R. Khanna, "A Two-Element MIMO Antenna for Sub-6 GHz and mmWave 5G Systems Using Characteristics Mode Analysis", *Microw. Opt. Technol. Lett.*, vol. 63, no. 2, pp. 587-595, 2021.

[13] N. Agrawal, M. Gupta and S. Chouhan, "Miniaturized Micro-strip Antenna for 5th Generation Applications", In Proceedings of the IEEE 4th International Conference on Electronics, Communication and Aerospace Technology (ICECA), 2020, pp. 592-595.

[14] E. Al-Abbas, M. Ikram, A. T. Mobashsher and A. Abbosh, "MIMO Antenna System for Multi-Band Millimeter-Wave 5G and Wideband 4G Mobile Communications", *IEEE Access*, vol. 7, pp. 181916-181923, Dec. 2019.

[15] Z. Wani, M. P. Abegaonkar and S. K. Koul, "A 28-GHz Antenna for 5G MIMO Applications", *Prog. Electromagn. Res. Lett.*, vol. 78, pp. 73-79, 2018.

[16] L. D. Malviya and P. Gupta P, "Millimeter Wave High-Gain Antenna Array for Wireless Applications", *IETE J. Res.*, vol. 69, no. 5, pp. 2645-2654, July 2023.

[17] A. Patel, A. Desai, I. Elfergani, A. Vala, H. Mewada, K. Mahant, S. Patel, C. Zebiri, J. Rodriguez and E. Ali, "UWB CPW Fed 4-port Connected Ground MIMO Antenna for Sub-Millimeter-Wave 5G Applications", *Alexandria Eng. J.*, vol. 61, no. 9, pp. 6645-6658, Sept. 2022.

[18] M. A. Khan, A. G. Al Harbi, S. H. Kiani, A. N. Nordin, M. E. Munir, S. I. Saeed, J. Iqbal, E. M. Ali, M. Alibakhshikenari and M. Dalarsson, "mmWave Four-Element MIMO Antenna for Future 5G Systems", *Appl. Sci.*, vol. 12, no. 9, p. 4280, Apr. 2022.
[19] H. Singh, B. Sohi and A. Gupta, "Designing and Performance Evaluation of Metamaterial Inspired Antenna for 4G and 5G applications", *Int. J. Electron.*, vol. 108, no. 6, pp. 1035-1057, 2020.
[20] R. Azim, A. Meaze, A. Affandi, M. Alam, R. Aktar, M. Mia and M. Islam, "A Multi-Slotted Antenna for LTE/5G Sub-6 GHz Wireless Communication Applications", *Int. J. Microw. Wirel. Technol.*, vol. 13, no. 5, pp. 486-496, 2021.
[21] I. Ishteyaq, I. Shah Masoodi and K. Muzaffar, "A Compact Double Band Planar Printed Slot Antenna for Sub-6 GHz 5G Wireless Applications", *Int. J. Microw. Wirel. Technol.*, vol. 13, no. 5, 469-477, 2021.
[22] N. Agrawal, M. Gupta and S. Chouhan, "Modified Ground and Slotted MIMO Antennas for 5G Sub-6 GHz Frequency Bands", *Int. J. Microw. Wirel. Technol.*, vol. 15, no. 5, pp. 817-825, 2022.
[23] A. K. Saurabh and M. K. Meshram, "Compact Sub-6 GHz 5G-Multiple-Input-Multiple-Output Antenna System with Enhanced Isolation", *Int. J. RF Microw. Computer-Aided Eng.*, vol. 30, no. 8, p. e22246, Aug. 2020.
[24] S. Chouhan, D. K. Panda, V. S. Kushwah and P. K. Mishra, "Octagonal-Shaped Wideband MIMO Antenna for Human Interface Device and S-band Application", *Int. J. Microw. Wirel. Technol.*, vol. 11, pp. 287-296, 2019.
[25] N. Agrawal, S. Chouhan and M. Gupta, "Quad Port Meander Line MIMO Antenna with the Stepped Ground Structure for 5G Wireless Application", In Proceedings of the IEEE 6th Conference on Information and Communication Technology (CICT), 2022, pp. 1-5.
[26] N. Agrawal, M. Gupta and S. Chauhan, "Design and Simulation of MIMO Antenna for Low Frequency 5G Band Application", In Proceedings of the IEEE 2nd Global Conference for Advancement in Technology (GCAT) Banglore, 2021, pp. 1-4.
[27] N. Agrawal, "A Comparative Study of UWB Micro-strip Antenna for Wireless Communication and RF Energy Harvesting", *IOP Conf. Ser.: Mater. Sci. Eng.*, vol. 1116, p. 012062, 2021.
[28] N. Agrawal and M. Gupta M, "Isolation Enhancement Techniques for UWB-MIMO System: A Review", In Proceedings of IEEE International Conference on Power Electronics & IoT Applications in Renewable Energy and its Control (PARC), 2020, pp. 113-117.
[29] S. Chouhan, D. K. Panda, M. Gupta and S. Singhal, "Multiport MIMO Antennas with Mutual Coupling Reduction Techniques for Modern Wireless Transreceive Operations: A Review", *Int. J. RF Microw. Computer-Aided Eng.*, vol. 28, no. 2, p. e21189, 2018.
[30] H. Ullah and F. A. Tahir, "A Broadband Wire Hexagon Antenna Array for Future 5G Communications in 28 GHz Band", *Microw. Opt. Technol. Lett.*, vol. 61, no. 13, pp. 696-701, 2019.
[31] P. Ranjan, S. Yadav and A. Bage, "Dual Band MIMO Antenna for LTE, 4G and Sub–6 GHz 5G Applications", *Facta Universitatis Series Electronics and Energetics.*, vol. 36, no. 1, pp. 43-51, 2023.
[32] A. Khan and J. S. Roy, "Design of Thinned Smart Antenna of Semi-circular Dipole Array for 5G Massive MIMO System", *Facta Universitatis Series Electronics and Energetics*, vol. 37, no. 3, pp. 409-422, Sept. 2024.
[33] S. Al-Bawri et al., "A High-Performance 3D Eight-Port THz-MIMO Antenna System Verified with Machine Learning for Enhanced Wireless Communication Systems", *Int. J. Commun. Syst.*, vol. 38, no. 4, p. e6006, 2024.
[34] A. Khan and J. S. Roy, "Thinned Smart Antenna of a Semi-circular Dipole Array for Massive MIMO Systems", *Adv. Electromagn.*, vol. 12, no. 4, pp. 17-25, Dec. 2023.